ORGANIC CHEMISTRY FRONTIERS

RESEARCH ARTICLE

View Article Online
View Journal | View Issue

Cite this: *Org. Chem. Front.*, 2026, **13**, 2279

B-spiroBODIPYs as a fluorophore responsive to hydrogen bond donors

Aiko Kondo,[a] Hideaki Takano *[a,b] and Hiroshi Shinokubo *[a,c,d]

Received 27th January 2026,
Accepted 23rd February 2026

DOI: 10.1039/d6qo00102e

rsc.li/frontiers-organic

Boron dipyrromethene (BODIPY) dyes possess excellent photophysical properties and are extensively used in chemical biology and materials science. While peripheral functionalisation of the dipyrromethene core is well established, modification at the boron centre has remained limited. Here, we demonstrate an Au-catalysed modulation of the boron centre, enabling the synthesis of B-spiroBODIPYs with a 1,3-dioxinone moiety on boron. The resulting B-spiroBODIPY exhibits solvent-dependent fluorescence arising from hydrogen-bonding interactions at the carbonyl oxygen on the 1,3-dioxinone moiety, offering a versatile platform for stimulus-responsive fluorescent probes.

Introduction

Boron dipyrromethene (BODIPY) and its derivatives are attractive organic dyes that display intense visible-light absorption and bright emission with high quantum yields.[1] Owing to these properties, BODIPY dyes have been widely applied in chemical biology and materials science.[2] BODIPY derivatives with appropriate functional groups can alter their photophysical properties in response to external stimuli such as pH,[3] temperature,[4] polarity[4a,5] and viscosity.[4a,6]

The introduction of functional groups onto the BODIPY unit has been conducted based on the versatile reactivity of the dipyrromethene skeleton. The peripheral positions of the BODIPY unit can be selectively manipulated through reactions with electrophiles, nucleophiles, radicals and transition metal catalysts, enabling precise modulation of their physical properties (Fig. 1a).[7]

On the other hand, functionalisation of the boron centre of BODIPY offers an attractive alternative strategy. It enables incorporation of additional features, including enhanced stability, solubility and modulated aggregation behaviour, while leaving the inherent optical properties of the BODIPY scaffold essentially intact (Fig. 1a).[8] However, the modification of the boron centre of the BODIPY unit has not been explored until recently.

The strategies for boron functionalisation can be divided into two types: one involves nucleophilic substitution on the boron atom,[9] and the other is B–O bond cleavage by photoirradiation.[10] In the case of nucleophilic substitution, the use of hard Lewis acids[9] or hard nucleophiles[9] is required to install the substituents on the boron centre. In addition, only BODIPYs with (pseudo)halogens on boron can be employed.

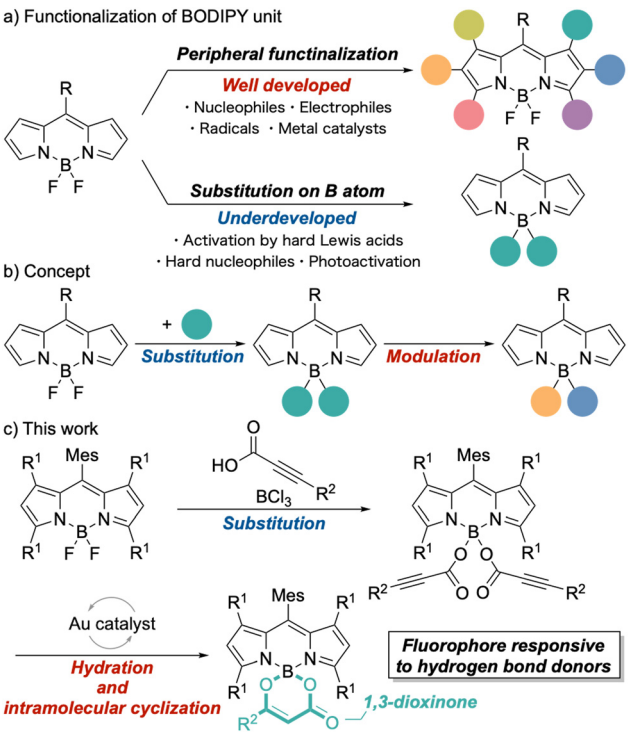

Fig. 1 Functionalisation of BODIPYs and the concept of this work.

[a]*Department of Molecular and Macromolecular Chemistry, Graduate School of Engineering, Nagoya University, Chikusa-ku, Nagoya, Aichi 464-8603, Japan. E-mail: htakano@chembio.nagoya-u.ac.jp, hshino@chembio.nagoya-u.ac.jp*
[b]*Institute for Advanced Research, Nagoya University, Furo-cho, Chikusa-ku, Nagoya, Aichi 464-8601, Japan*
[c]*Research Institute for Quantum and Chemical Innovation, Institutes of Innovation for Future Society, Furo-cho, Chikusa-ku, Nagoya, Aichi 464-8601, Japan*
[d]*Integrated Research Consortium on Chemical Science (IRCCS), Furo-cho, Chikusa-ku, Nagoya, Aichi 464-8602, Japan*

Photoinduced B–O bond cleavage of O-BODIPY can generate the corresponding borenium cation, which is utilised as a photocage in cell biology.[10] However, only hydroxy and alkoxy groups from solvents can be introduced on the boron centre.

In this work, we advance the concept of modulating BODIPY properties by reconfiguring its boron coordination environment. Further transformations of substituents on the boron centre provide a versatile strategy for introducing new functionalities and tuning the behaviour of BODIPY dyes (Fig. 1b). Herein, we have successfully developed an Au-catalysed modulation at the boron centre of COO-BODIPY, affording B-spiroBODIPYs with a 1,3-dioxinone moiety on the boron centre (Fig. 1c). The obtained B-spiroBODIPY exhibits solvent-dependent fluorescence through hydrogen bonding between its carbonyl oxygen and solvent molecules, underscoring its potential as a stimulus-responsive fluorescent probe.[11]

Results and discussion

We first synthesised COO-BODIPY **2a** derivatives from F-BODIPY **1a** with corresponding carboxylic acids in the presence of BCl_3 and triethylamine (Scheme 1).[9] Treatment of **2a** with the combination of AuCl(IPr) (IPr = 1,3-bis(2,6-diisopropylphenyl)imidazol-2-ylidene) and silver triflate in the presence of tetrabutylammonium triflate afforded B-spiroBODIPY **3a** in 80% yield (Scheme 1).[12] This protocol was applied to BODIPY **2b** and tetramethylBODIPY **2c**, providing corresponding B-spiroBODIPYs **3b** and **3c** in 92% and 75% yields, respectively.

The structure of **3a** was unambiguously determined by X-ray crystal analysis (Fig. 2). The single crystal of **3a** was obtained by vapour diffusion of hexane to a solution of **3a** in dichloromethane. In BODIPY **3a**, the 1,3-dioxinone moiety is orthogonal to a BODIPY subunit. The mean plane deviation (MPD) of the BODIPY subunit was 0.031 Å, indicating that the spiro structure did not affect the planarity of the BODIPY core. It is worth noting that the distance between a carbon atom in dichloromethane and an oxygen atom at the carbonyl group

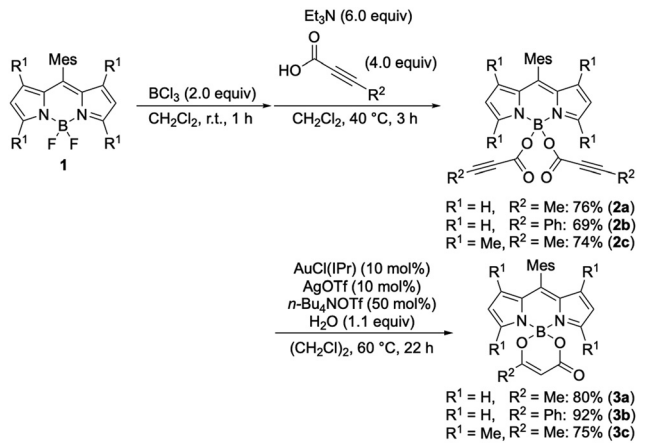

Scheme 1 Synthesis of B-spiroBODIPY **3** *via* Au-catalysed hydration and cyclisation.

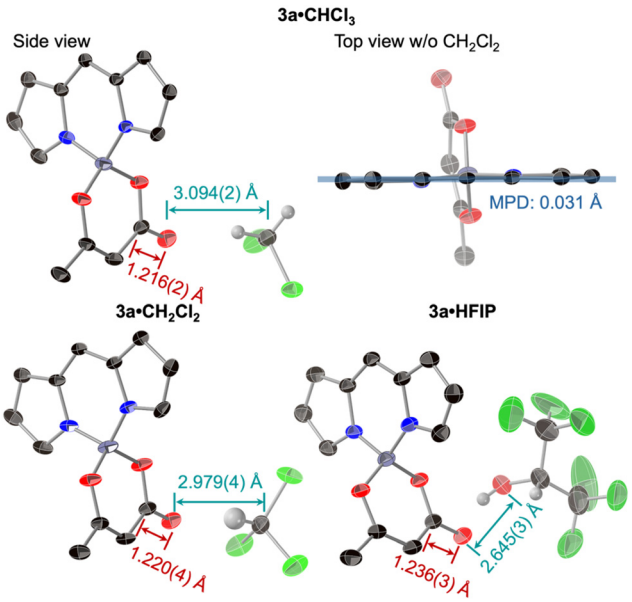

Fig. 2 X-ray crystal structures of **3a·CH_2Cl_2**, **3a·$CHCl_3$** and **3a·HFIP**. Thermal ellipsoids are shown at 50% probability. Hydrogen atoms, except for those in solvents, and mesityl groups are omitted for clarity.

was 3.094 Å, which was shorter than the sum of van der Waals radii of carbon (1.70 Å) and oxygen (1.52 Å). These results suggest that the carbonyl group in **3a** forms hydrogen bonding with dichloromethane co-crystallised in the crystal **3a·CH_2Cl_2**. Single crystals **3a·$CHCl_3$** and **3a·HFIP** were also obtained by evaporation of a chloroform solution of **3a** and vapour diffusion of water into a solution of **3a** in 1,1,1,3,3,3-hexafluoroisopropan-2-ol (HFIP). The distance between the carbon atom of chloroform and the carbonyl oxygen was 2.979 Å, whereas the distance between the oxygen atom of HFIP and the carbonyl oxygen was 2.645 Å. Furthermore, the C=O bond lengths in **3a·CH_2Cl_2**, **3a·$CHCl_3$** and **3a·HFIP** were 1.216 Å, 1.220 Å and 1.236 Å, respectively. These findings indicate that **3a** interacts tightly with HFIP through hydrogen bonding with its carbonyl oxygen.[13]

We examined the functionalisation of the obtained B-spiroBODIPY derivatives **3** (Scheme 2). The reaction of **3a**

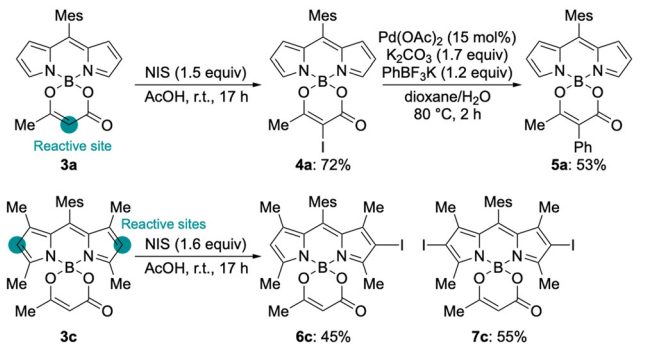

Scheme 2 Functionalisation of B-spiroBODIPY **3**.

with *N*-iodosuccinimide (NIS) in acetic acid promoted selective iodination on the central carbon atom of the 1,3-dioxinone moiety in 72% yield.[14] The subsequent Suzuki–Miyaura coupling of **4a** provided the arylated product **5a** in 53% yield. In sharp contrast, iodination of **3c** proceeded on the BODIPY subunit under the same conditions to afford mono- and di-iodinated BODIPY **6c** and **7c** in 45% and 55% yield, respectively. These results suggest that the most nucleophilic site is on the 1,3-dioxinone moiety in **3a** but on the BODIPY framework in **3c**. These results demonstrated that regioselective functionalisation of B-spiroBODIPYs **3** enables further elaboration of the BODIPY and 1,3-dioxinone moieties to fine-tune their properties.

We measured absorption and emission spectra of COO-BODIPY **2a** and B-spiroBODIPYs **3** in CH_2Cl_2 (Fig. 3). Both COO-BODIPY **2a** and B-spiroBODIPYs **3** exhibit intense absorption bands around 505 nm and emission bands around 520 nm, regardless of the substituent on the boron atoms. The absorption and fluorescence spectral shapes of **2a** and **3** are comparable to those of BODIPY **1a**.[15] However, the quantum yields Φ_F of **3a** and **3b** were 0.078 and 0.069, respectively, which are markedly different from those of **2a** (Φ_F = 0.74) and **3c** (Φ_F = 0.79), demonstrating the efficient photophysical modulation by functionalisation at the boron centre. The decrease in fluorescence quantum yield can be explained by intramolecular charge transfer from the electron-donating 1,3-dioxinone moiety to the electron-accepting BODIPY subunit.

We evaluated the solvent effect on the photophysical properties of **3a** (Table 1). The shape of the absorption and emission spectra displayed almost no change in various solvents (Fig. S41 and S42). However, the emission quantum yield was significantly modulated by the solvents. In chloroform, the quantum yield increased to 0.30 compared to that in CH_2Cl_2 (0.078). While the fluorescence intensities were comparable in apolar solvents such as CH_2Cl_2, toluene, hexane and Et_2O, fluorescence became slightly stronger in alcohols. We hypothesise that hydrogen bond donors interact with the carbonyl oxygen on the 1,3-dioxinone moiety, thereby enhancing the fluorescence. We then chose HFIP as a strong hydrogen bond donor,[13] which dramatically enhanced the fluorescence quantum yield to 0.93. In addition, we measured absorption and emission in the presence of water in acetonitrile (Fig. 4). As water content increased, the emission quantum yield was enhanced from 0.019 to 0.16. This result can also be attributed to the hydrogen bonding interaction with water.

We also determined fluorescence lifetimes in different solvents to estimate the rates of radiative and non-radiative decay. The fluorescence decay profiles were fitted with a double-exponential function to determine the average fluorescence lifetimes (Fig. S43 and S44). While the fluorescence lifetimes in toluene and CH_2Cl_2 were 1.7 ns and 1.1 ns, respectively, that in HFIP was much longer (10.4 ns). The k_f value in Et_2O was an order of magnitude smaller, resulting in significantly reduced fluorescence intensity. The k_f values were comparable in other solvents. However, the k_{nr} value in HFIP was one hundredth of the value measured in other solvents. We considered that hydrogen bonding stabilises the molecular orbital of the

Table 1 Photophysical properties of **3a** in various solvents

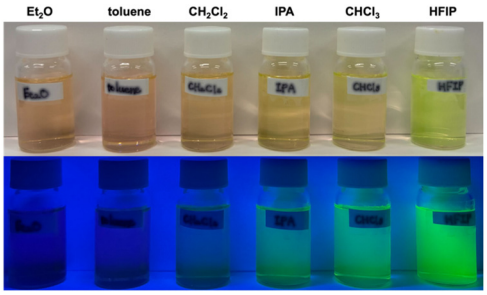

Solvent	Φ_F	$\langle\tau\rangle$/ns	$k_f/10^7$ s^{-1}	$k_{nr}/10^8$ s^{-1}
Et_2O	0.030	3.8	0.79	2.5
toluene	0.071	1.7	4.2	5.5
CH_2Cl_2	0.078	1.1	6.8	8.0
IPA	0.22	3.0	7.3	2.6
$CHCl_3$	0.30	4.5	6.7	1.6
HFIP	0.93	10.4	9.0	0.067

Quantum yields and fluorescence lifetimes were obtained with 10^{-5} M solutions.

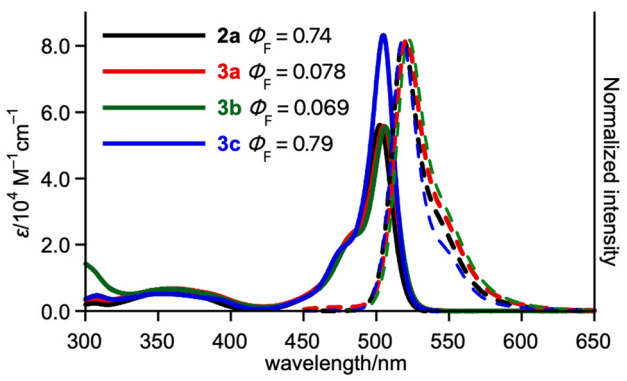

Fig. 3 Absorption and emission spectra of **2a** and **3** in CH_2Cl_2. Absorption and fluorescence spectra were measured with 10^{-5} M solutions.

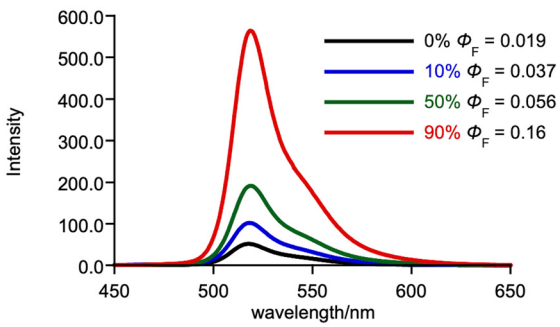

Fig. 4 Fluorescence spectra in MeCN–H_2O mixture containing *X*% (w/w) H_2O (*X* = 0, 10, 50, 90).

1,3-dioxinone moiety, thus suppressing intramolecular charge transfer leading to non-radiative decay.

To verify the presence of hydrogen bonding in solution, we measured the infrared absorption spectra of **3a** in various solutions to evaluate the carbonyl stretching vibration (Fig. 5). In Et_2O, where the fluorescence quantum yield was the lowest, the C=O stretching vibration was observed at 1716 cm^{-1}. As the fluorescence quantum yield increased, the C=O stretching band shifted to lower wavenumbers. The C=O stretching vibration peak was detected at 1632 cm^{-1} in HFIP. These observations clearly indicate that the carbonyl group of **3a** forms hydrogen bonds with the solvent.

To gain a deeper insight into the solvent effect on **3a**, we conducted DFT calculations.[16] The structure optimisations were conducted at the B3LYP/6-31+G(d,p) level of theory (Fig. 6). The single-point calculations were performed at the B3LYP/6-311+G(d,p) level of theory using the optimised structure or the crystal structure. Both HOMO and LUMO of **2a** were localised on the BODIPY subunit, which were almost identical with those of BODIPY **1a**.[17] Conversely, the HOMO (−6.33 eV) and HOMO−1 (−6.42 eV) of **3a** were almost degenerated, which were delocalised on both BODIPY and 1,3-dioxinone subunits. These differences in molecular orbitals contributed to the photophysical properties before and after spiro cyclisation. The LUMO of **3a** was rather localised on the BODIPY subunit. Therefore, the partial orbital separation in **3a** indicates the existence of intramolecular charge transfer character in the excited state, which contributes to its less emissive feature. In contrast, the HOMO and LUMO of **3c** were destabilised by electron-donating methyl groups, resulting in lifting the degeneracy between the HOMO (−5.74 eV) and HOMO−1 (−6.30 eV). Accordingly, the HOMO and LUMO of **3c** were almost identical with those of BODIPY **1a** and **2a**, resulting in the retrieval of the emissive nature of BODIPY.

The dihedral angles between the mean planes of the BODIPY and 1,3-dioxinone subunits were 83.0° and 90.0° in the optimized structures of **3a** and **3c**, respectively. We concluded that the dihedral angles did not significantly affect the degeneracy of the HOMO and HOMO−1. The difference in the frontier orbitals of **3a** and **3c** can also explain the regioselectivity of electrophilic iodination observed in Scheme 2. The HOMO of **3a** exhibits high MO coefficients on the 1,3-dioxinone subunit, which undergoes the electrophilic iodination. In contrast, the HOMO of **3c** is mainly located on the BODIPY subunit, resulting in β-selective iodination of the BODIPY core.

In the crystal structure of **3a·HFIP**, the degeneracy between HOMO and HOMO−1 was lifted, as the molecular orbital derived from the 1,3-dioxinone subunit was substantially stabilised by hydrogen bonding. Consequently, the effect of intramolecular charge transfer was almost diminished in **3a·HFIP**, thus improving its fluorescence intensity.

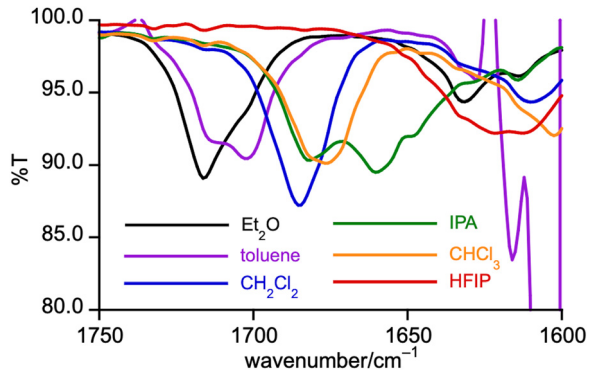

Fig. 5 IR spectrum of **3a** in various solvents (*ca.* 0.6 mM).

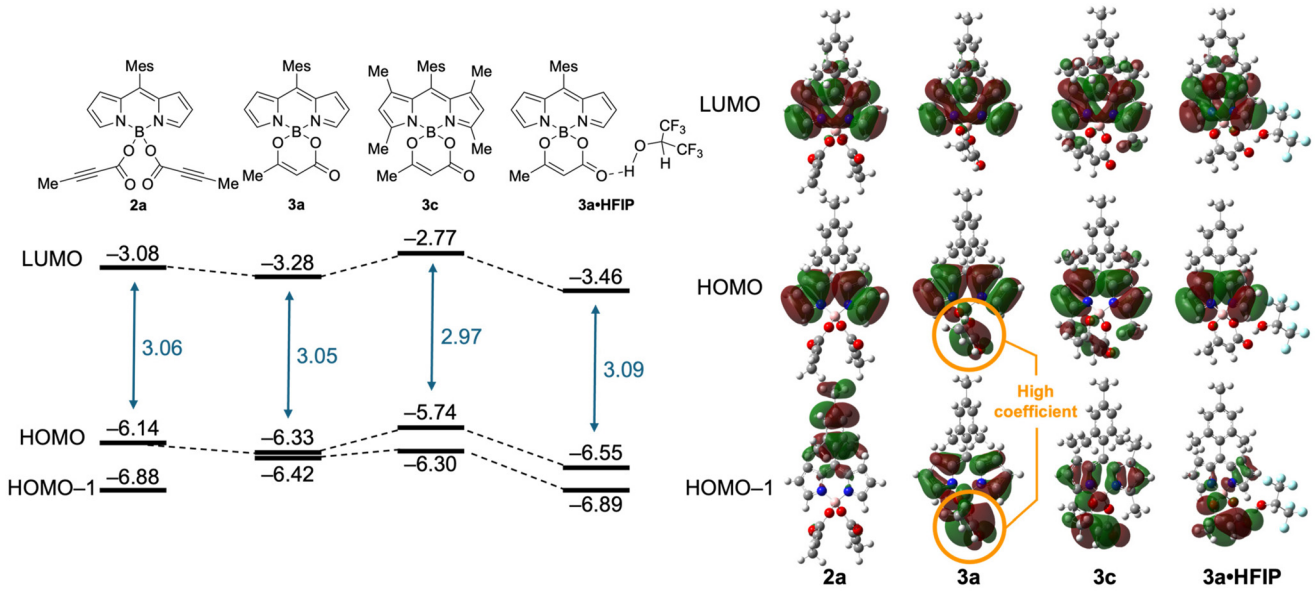

Fig. 6 Molecular orbitals of COO-BODIPY **2a** and B-spiroBODIPY **3a**, **3c**, and **3a·HFIP** (unit: eV).

Conclusions

We developed the additional functionalisation of COO-BODIPY **2** to synthesise B-spiroBODIPY *via* an Au-catalysed hydration and subsequent intramolecular cyclisation. B-spiroBODIPY **3** possessed a 1,3-dioxinone moiety, which can be further transformed by halogenation and cross-coupling reaction. While B-spiroBODIPY **3a** exhibited very weak fluorescence in non-hydrogen-bonding solvents, its photophysical properties, including a quantum yield and fluorescence lifetime, were remarkably modulated by hydrogen bond donors. B-spiroBODIPYs with a 1,3-dioxinone subunit are promising as an environment-sensitive dye for fluorescence lifetime imaging microscopy and would be useful in the field of chemical biology.[6a,b,18]

Author contributions

H. T. and H. S. designed and conducted the project, prepared the original draft, and finalised the manuscript. A. K. carried out all the experiments, including the synthesis and characterisation. The manuscript was written with contributions from all authors. All authors have approved the final version of the manuscript.

Conflicts of interest

There are no conflicts to declare.

Data availability

The data supporting this article have been included as part of the supplementary information (SI). Supplementary information: Fig. S41–S44, NMR spectra, HR-MS spectra, further experimental details and calculation details. See DOI: **https://doi.org/10.1039/d6qo00102e**.

CCDC 2523317–2523319 for **3a·CHCl$_3$**, **3a·HFIP** and **3a·CH$_2$Cl$_2$** contain the supplementary crystallographic data for this paper.[19a–c]

Acknowledgements

This work was supported by the Japan Society for the Promotion of Science (JSPS) *via* KAKENHI grants JP20H05862, JP20H05863, JP22H04974 and JP24K17675. This work was also supported by MEXT (Japan) *via* the Leading Initiative for Excellent Young Researchers (grant: JPMXS0320220200). H. T. acknowledges the Hibi Science Foundation for financial support. We gratefully acknowledge Prof. Shigehiro Yamaguchi and Prof. Soichiro Ogi (Nagoya University) for their assistance with the solution-phase IR spectroscopy measurements.

References

1 (*a*) G. Ulrich, R. Ziessel and A. Harriman, The Chemistry of Fluorescent Bodipy Dyes: Versatility Unsurpassed, *Angew. Chem., Int. Ed.*, 2008, **47**, 1184–1201; (*b*) J. Bañuelos, BODIPY Dye, the Most Versatile Fluorophore Ever?, *Chem. Rec.*, 2016, **16**, 335–348; (*c*) A. Loudet and K. Burgess, BODIPY Dyes and Their Derivatives: Syntheses and Spectroscopic Properties, *Chem. Rev.*, 2007, **107**, 4891–4932.

2 (*a*) D. Li, H. Zhang and Y. Wang, Four-Coordinate Organoboron Compounds for Organic Light-Emitting Diodes (OLEDs), *Chem. Soc. Rev.*, 2013, **42**, 8416–8433; (*b*) A. Bessette and G. S. Hanan, Design, Synthesis and Photophysical Studies of Dipyrromethene-Based Materials: Insights into Their Applications in Organic Photovoltaic Devices, *Chem. Soc. Rev.*, 2014, **43**, 3342–3405; (*c*) T. Kowada, H. Maeda and K. Kikuchi, BODIPY-Based Probes for the Fluorescence Imaging of Biomolecules in Living Cells, *Chem. Soc. Rev.*, 2015, **44**, 4953–4972; (*d*) H. Klfout, A. Stewart, M. Elkhalifa and H. He, BODIPYs for Dye-Sensitized Solar Cells, *ACS Appl. Mater. Interfaces*, 2017, **9**, 39873–39889; (*e*) C. Ripoll, C. Cheng, E. Garcia-Fernandez, J. Li, A. Orte, H. Do, L. Jiao, D. Robinson, L. Crovetto, J. A. González-Vera, E. M. Talavera, J. M. Alvarez-Pez, N. Boens and M. J. Ruedas-Rama, Synthesis and Spectroscopy of Benzylamine-Substituted BODIPYs for Bioimaging, *Eur. J. Org. Chem.*, 2018, 2561–2571; (*f*) P. Kaur and K. Singh, Recent Advances in the Application of BODIPY in Bioimaging and Chemosensing, *J. Mater. Chem. C*, 2019, **7**, 11361–11405; (*g*) M. Poddar and R. Misra, Recent Advances of BODIPY Based Derivatives for Optoelectronic Applications, *Coord. Chem. Rev.*, 2020, **421**, 213462; (*h*) L. Yuan, Y. Su, H. Cong, B. Yu and Y. Shen, Application of Multifunctional Small Molecule Fluorescent Probe BODIPY in Life Science, *Dyes Pigm.*, 2023, **208**, 110851; (*i*) D. Spector, D. S. Abramchuk, V. V. Bykusov, A. O. Zharova, E. S. Egorova, A. S. Voskresenskaya, A. R. Olovyanishnikov, I. A. Kuzmichev, A. A. Bubley, R. L. Antipin, E. Beloglazkina and O. Krasnovskaya, BODIPY: Synthesis, Modification, and Applications in Sensing and Biomedicine, *Russ. Chem. Rev.*, 2024, **93**, RCR5136.

3 (*a*) M. Kollmannsberger, T. Gareis, S. Heinl, J. Daub and J. Breu, Electrogenerated Chemiluminescence and Proton-Dependent Switching of Fluorescence: Functionalized Difluoroboradiaza-s-Indacenes, *Angew. Chem., Int. Ed. Engl.*, 1997, **36**, 1333–1335; (*b*) T. Gareis, C. Huber, O. S. Wolfbeis and J. Daub, Phenol/Phenolate-Dependent on/off Switching of the Luminescence of 4,4-Difluoro-4-Bora-3a,4a-Diaza-*s*-Indacenes, *Chem. Commun.*, 1997, 1717–1718; (*c*) C. N. Baki and E. U. Akkaya, Boradiazaindacene-Appended Calix[4] Arene: Fluorescence Sensing of pH Near Neutrality, *J. Org. Chem.*, 2001, **66**, 1512–1513; (*d*) M. Baruah, W. Qin, N. Basarić, W. M. De Borggraeve and N. Boens, BODIPY-Based Hydroxyaryl Derivatives as Fluorescent pH

Probes, *J. Org. Chem.*, 2005, **70**, 4152–4157; (*e*) W. Qin, M. Baruah, W. M. De Borggraeve and N. Boens, Photophysical Properties of an on/off Fluorescent pH Indicator Excitable with Visible Light Based on a Borondipyrromethene-Linked Phenol, *J. Photochem. Photobiol., A*, 2006, **183**, 190–197.

4 (*a*) A. Vyšniauskas, M. Qurashi, N. Gallop, M. Balaz, H. L. Anderson and M. K. Kuimova, Unravelling the Effect of Temperature on Viscosity-Sensitive Fluorescent Molecular Rotors, *Chem. Sci.*, 2015, **6**, 5773–5778; (*b*) H. Wang, Y. Wu, Y. Shi, P. Tao, X. Fan, X. Su and G.-C. Kuang, BODIPY-Based Fluorescent Thermometer as a Lysosome-Targetable Probe: How the Oligo(Ethylene Glycols) Compete Photoinduced Electron Transfer, *Chem. – Eur. J.*, 2015, **21**, 3219–3223; (*c*) A. Vyšniauskas, I. López-Duarte, N. Duchemin, T.-T. Vu, Y. Wu, E. M. Budynina, Y. A. Volkova, E. P. Cabrera, D. E. Ramírez-Ornelas and M. K. Kuimova, Exploring Viscosity, Polarity and Temperature Sensitivity of BODIPY-Based Molecular Rotors, *Phys. Chem. Chem. Phys.*, 2017, **19**, 25252–25259; (*d*) M. M. Ogle, A. D. Smith McWilliams, M. J. Ware, S. A. Curley, S. J. Corr and A. A. Martí, Sensing Temperature in Vitro and in Cells Using a BODIPY Molecular Probe, *J. Phys. Chem. B*, 2019, **123**, 7282–7289; (*e*) M. C. de Souza, J. V. M. de Jesus, L. F. Pedrosa, I. P. Gomes, F. Duarte, C. I. M. Santos, C. Lodeiro, M. G. P. M. S. Neves, J. A. S. Cavaleiro, R. F. Mendes and F. A. A. Paz, Multifunctional BODIPY-Based Fluorophores for Temperature Detection: Synthesis, Structure, and Performance, *Dyes Pigm.*, 2026, **246**, 113427.

5 (*a*) M. Kollmannsberger, K. Rurack, U. Resch-Genger and J. Daub, Ultrafast Charge Transfer in Amino-Substituted Boron Dipyrromethene Dyes and Its Inhibition by Cation Complexation: A New Design Concept for Highly Sensitive Fluorescent Probes, *J. Phys. Chem. A*, 1998, **102**, 10211–10220; (*b*) H. Sunahara, Y. Urano, H. Kojima and T. Nagano, Design and Synthesis of a Library of BODIPY-Based Environmental Polarity Sensors Utilizing Photoinduced Electron-Transfer-Controlled Fluorescence ON/OFF Switching, *J. Am. Chem. Soc.*, 2007, **129**, 5597–5604; (*c*) Y. Bai, X. Shi, Y. Chen, C. Zhu, Y. Jiao, Z. Han, W. He and Z. Guo, Coumarin/BODIPY Hybridisation for Ratiometric Sensing of Intracellular Polarity Oscillation, *Chem. – Eur. J.*, 2018, **24**, 7513–7524.

6 (*a*) M. K. Kuimova, G. Yahioglu, J. A. Levitt and K. Suhling, Molecular Rotor Measures Viscosity of Live Cells via Fluorescence Lifetime Imaging, *J. Am. Chem. Soc.*, 2008, **130**, 6672–6673; (*b*) J. A. Levitt, M. K. Kuimova, G. Yahioglu, P.-H. Chung, K. Suhling and D. Phillips, Membrane-Bound Molecular Rotors Measure Viscosity in Live Cells via Fluorescence Lifetime Imaging, *J. Phys. Chem. C*, 2009, **113**, 11634–11642; (*c*) I. López-Duarte, T. T. Vu, M. A. Izquierdo, J. A. Bull and M. K. Kuimova, A Molecular Rotor for Measuring Viscosity in Plasma Membranes of Live Cells, *Chem. Commun.*, 2014, **50**, 5282–5284.

7 (*a*) V. Lakshmi, R. Sharma and M. Ravikanth, Functionalized Boron-Dipyrromethenes and Their Applications, *Rep. Org. Chem.*, 2016, **6**, 1–24; (*b*) N. Boens, B. Verbelen, M. J. Ortiz, L. Jiao and W. Dehaen, Synthesis of BODIPY Dyes through Postfunctionalization of the Boron Dipyrromethene, *Coord. Chem. Rev.*, 2019, **399**, 213024; (*c*) F. Ma, L. Zhou, Q. Liu, C. Li and Y. Xie, Selective Photocatalysis Approach for Introducing ArS Units into BODIPYs through Thiyl Radicals, *Org. Lett.*, 2019, **21**(3), 733–736; (*d*) J. Labella, G. Durán-Sampedro, M. V. Martínez-Díaz and T. Torres, Annulative π-Extension of BODIPYs Made Easy via Gold(I)-Catalyzed Cycloisomerization, *Chem. Sci.*, 2020, **11**, 10778–10785; (*e*) T. Shimada, S. Mori, M. Ishida and H. Furuta, Regioselectively α- and β-Alkynylated BODIPY Dyes via Gold (I)-catalyzed Direct C–H Functionalization and Their Photophysical Properties, *Beilstein J. Org. Chem.*, 2020, **16**, 587–595; (*f*) D. Wang, L. Wang, X. Guo, X. Zhang, J. Ma, Z. Kang, Z.-Y. Li, L. Jiao and E. Hao, Visible-Light-Induced Direct Photoamination of BODIPY Dyes with Aqueous Ammonia, *Org. Lett.*, 2023, **25**, 7650–7655; (*g*) H. Shu, M. Guo, M. Wang, S. Fan, M. Zhou, L. Xu, Y. Rao, A. Osuka and J. Song, Rhodium-Catalyzed [5 + 2] Annulation of Pyrrole Appended BODIPYs: Access to Azepine-Fused BODIPYs, *Org. Lett.*, 2023, **25**, 1817–1822; (*h*) X.-X. Dong, J.-G. Liu, H.-X. Zhang and B. Zhang, A Practical and Modular Method for Direct C–H Functionalization of the BODIPY Core via Thianthrenium Salts, *Chem. – Eur. J.*, 2024, **30**, e202401929; (*i*) A. D. Lama, J. P. Sestelo, L. A. Sarandeses and M. M. Martínez, Synthesis and Photophysical Properties of β-Alkenyl-Substituted BODIPY Dyes by Indium(III)-Catalyzed Intermolecular Alkyne Hydroarylation, *J. Org. Chem.*, 2024, **89**, 4702–4711; (*j*) F. Ohashi, H. Takano and H. Shinokubo, Zig-zag-fused π-Extended BODIPYs via Gold-catalysed Cycloisomerisation, *Chem. Commun.*, 2024, **60**, 12892–12895; (*k*) M. Wang, S. Fan, C. Duan, H. Shu, R. Ding, M. Zhou, L. Xu, Y. Rao, A. Osuka and J. Song, Rhodium-Catalyzed Regioselective Alkynylations of 8-Pyrrole-appended BODIPYs, *Org. Chem. Front.*, 2024, **11**, 5798–5805.

8 M. Bogomolec, M. Glavaš, I. Škorić, M. Bogomolec, M. Glavaš and I. Škorić, BODIPY Compounds Substituted on Boron, *Molecules*, 2024, **29**, 5157.

9 (*a*) G. Ulrich, C. Goze, S. Goeb, P. Retailleau and R. Ziessel, New Fluorescent Aryl- or Ethynylaryl-Boron-Substituted Indacenes as Promising Dyes, *New J. Chem.*, 2006, **30**, 982–986; (*b*) C. Tahtaoui, C. Thomas, F. Rohmer, P. Klotz, G. Duportail, Y. Mély, D. Bonnet and M. Hibert, Convenient Method To Access New 4,4-Dialkoxy- and 4,4-Diaryloxy-Diaza-*s*-Indacene Dyes: Synthesis and Spectroscopic Evaluation, *J. Org. Chem.*, 2007, **72**, 269–272; (*c*) C. Bonnier, W. E. Piers, A. Al-Sheikh Ali, A. Thompson and M. Parvez, Perfluoroaryl-Substituted Boron Dipyrrinato Complexes, *Organometallics*, 2009, **28**, 4845–4851; (*d*) H. Manzano, I. Esnal, T. Marqués-Matesanz,

J. Bañuelos, I. López-Arbeloa, M. J. Ortiz, L. Cerdán, A. Costela, I. García-Moreno and J. L. Chiara, Unprecedented J-Aggregated Dyes in Pure Organic Solvents, *Adv. Funct. Mater.*, 2016, **26**, 2756–2769; (*e*) K. Yuan, X. Wang, S. K. Mellerup, I. Kozin and S. Wang, Spiro-BODIPYs with a Diaryl Chelate: Impact on Aggregation and Luminescence, *J. Org. Chem.*, 2017, **82**, 13481–13487; (*f*) G. Zhang, M. Wang, F. R. Fronczek, K. M. Smith and M. G. H. Vicente, Lewis-Acid-Catalyzed BODIPY Boron Functionalization Using Trimethylsilyl Nucleophiles, *Inorg. Chem.*, 2018, **57**, 14493–14496; (*g*) C. Ray, C. Schad, F. Moreno, B. L. Maroto, J. Bañuelos, T. Arbeloa, I. García-Moreno, C. Villafuerte, G. Muller and S. de la Moya, BCl_3-Activated Synthesis of COO-BODIPY Laser Dyes: General Scope and High Yields under Mild Conditions, *J. Org. Chem.*, 2020, **85**, 4594–4601; (*h*) C. Ray, E. Avellanal-Zaballa, M. Muñoz-Úbeda, J. Colligan, F. Moreno, G. Muller, I. López-Montero, J. Bañuelos, B. L. Maroto and S. de la Moya, Dissimilar-at-Boron *N*-BODIPYs: From Light-Harvesting Multichromophoric Arrays to CPL-Bright Chiral-at-Boron BODIPYs, *Org. Chem. Front.*, 2023, **10**, 5834–5842.

10 (*a*) S. Shaban Ragab, S. Swaminathan, E. Deniz, B. Captain and F. M. Raymo, Fluorescence Photoactivation by Ligand Exchange around the Boron Center of a BODIPY Chromophore, *Org. Lett.*, 2013, **15**, 3154–3157; (*b*) N. Umeda, H. Takahashi, M. Kamiya, T. Ueno, T. Komatsu, T. Terai, K. Hanaoka, T. Nagano and Y. Urano, Boron Dipyrromethene As a Fluorescent Caging Group for Single-Photon Uncaging with Long-Wavelength Visible Light, *ACS Chem. Biol.*, 2014, **9**, 2242–2246; (*c*) P. Kumari, A. Kulkarni, A. K. Sharma and H. Chakrapani, Visible-Light Controlled Release of a Fluoroquinolone Antibiotic for Antimicrobial Photopharmacology, *ACS Omega*, 2018, **3**, 2155–2160; (*d*) K. Zlatić, M. Popović, L. Uzelac, M. Kralj and N. Basarić, Antiproliferative Activity of *Meso*-Substituted BODIPY Photocages: Effect of Electrophiles vs Singlet Oxygen, *Eur. J. Med. Chem.*, 2023, **259**, 115705; (*e*) K. C. Dissanayake, D. Yuan and A. H. Winter, Structure–Photoreactivity Studies of BODIPY Photocages: Limitations of the Activation Barrier for Optimizing Photoreactions, *J. Org. Chem.*, 2024, **89**, 6740–6748.

11 (*a*) J. Han, B. Cao, X. Zhang, X. Su, L. Diao, H. Yin and Y. Shi, Size Dependent Hydrogen-Bonded Methanol Wires Regulating the Fluorescence On-Off of 1-*H*-Pyrrolo[3,2-*h*] Quinoline·$(MeOH)_{n=1,2}$ Complexes with ESMPT, *J. Mol. Liq.*, 2020, **306**, 112894; (*b*) H. Zhan, Z. Tang, Z. Li, X. Chen, J. Tian, X. Fei and Y. Wang, The Influence of Intermolecular Hydrogen Bonds on Single Fluorescence Mechanism of 1-Hydroxy-11*H*-Benzo [b]Fluoren-11-One and 10-Hydroxy-11*H*-Benzo [b]Fluoren-11-One, *Spectrochim. Acta, Part A*, 2021, **260**, 119993; (*c*) A. Pal, I. Ahmad and N. Dey, Hydrogen-Bond-Assisted Dual-Mode Ratiometric Detection of Uric Acid Using Pyrimidine-Driven Charge Transfer Probes: From Mechanistic Studies to Real-Life Applications, *ACS Appl. Bio Mater.*, 2025, **8**, 4699–4706; (*d*) R. S. Fernandes and N. Dey, Exploring the Synergistic Effect of Aggregation and Hydrogen Bonding: A Fluorescent Probe for Dual Sensing of Phytic Acid and Uric Acid, *J. Mater. Chem. B*, 2024, **12**, 11789–11799.

12 W. Wang, M. Kumar, G. B. Hammond and B. Xu, Enhanced Reactivity in Homogeneous Gold Catalysis through Hydrogen Bonding, *Org. Lett.*, 2014, **16**, 636–639.

13 (*a*) W. J. Middleton and R. V. Lindsey, Hydrogen Bonding in Fluoro Alcohols, *J. Am. Chem. Soc.*, 1964, **86**, 4948–4952; (*b*) G. R. Wiley and S. I. Miller, Thermodynamic Parameters for Hydrogen Bonding of Chloroform with Lewis Bases in Cyclohexane. Proton Magnetic Resonance Study, *J. Am. Chem. Soc.*, 1972, **94**, 3287–3293; (*c*) F. L. Slejko, R. S. Drago and D. G. Brown, Failure of Some Commonly Accepted Spectroscopic-enthalpy Correlations for Chloroform Adducts, *J. Am. Chem. Soc.*, 1972, **94**, 9210–9216; (*d*) G. R. Desiraju, The C–H···O Hydrogen Bond: Structural Implications and Supramolecular Design, *Acc. Chem. Res.*, 1996, **29**, 441–449; (*e*) F. H. Allen, P. A. Wood and P. T. A. Galek, Role of chloroform and dichloromethane solvent molecules in crystal packing: an interaction propensity study, *Acta Crystallogr., Sect. B:Struct. Sci., Cryst. Eng. Mater.*, 2013, **69**, 379–388; (*f*) H. F. Motiwala, A. M. Armaly, J. G. Cacioppo, T. C. Coombs, K. R. K. Koehn, V. M. Norwood IV and J. Aubé, HFIP in Organic Synthesis, *Chem. Rev.*, 2022, **122**, 12544–12747.

14 S. Yeom and K. Ohmori, One-Pot Synthesis of Functionalized Benzotropones via a Phthalide Ring-Opening/Intramolecular Aldol Condensation Cascade, *Org. Lett.*, 2024, **26**, 5120–5124.

15 Y. Hayashi, S. Yamaguchi, W. Y. Cha, D. Kim and H. Shinokubo, Synthesis of Directly Connected BODIPY Oligomers through Suzuki–Miyaura Coupling, *Org. Lett.*, 2011, **13**, 2992–2995.

16 M. J. Frisch, G. W. Trucks, H. B. Schlegel, G. E. Scuseria, M. A. Robb, J. R. Cheeseman, G. Scalmani, V. Barone, G. A. Petersson, H. Nakatsuji, X. Li, M. Caricato, A. V. Marenich, J. Bloino, B. G. Janesko, R. Gomperts, B. Mennucci, H. P. Hratchian, J. V. Ortiz, A. F. Izmaylov, J. L. Sonnenberg, D. Williams-Young, F. Ding, F. Lipparini, F. Egidi, J. Goings, B. Peng, A. Petrone, T. Henderson, D. Ranasinghe, V. G. Zakrzewski, J. Gao, N. Rega, G. Zheng, W. Liang, M. Hada, M. Ehara, K. Toyota, R. Fukuda, J. Hasegawa, M. Ishida, T. Nakajima, Y. Honda, O. Kitao, H. Nakai, T. Vreven, K. Throssell, J. A. Montgomery, Jr., J. E. Peralta, F. Ogliaro, M. J. Bearpark, J. J. Heyd, E. N. Brothers, K. N. Kudin, V. N. Staroverov, T. A. Keith, R. Kobayashi, J. Normand, K. Raghavachari, A. P. Rendell, J. C. Burant, S. S. Iyengar, J. Tomasi, M. Cossi, J. M. Millam, M. Klene, C. Adamo, R. Cammi, J. W. Ochterski, R. L. Martin, K. Morokuma, O. Farkas, J. B. Foresman and D. J. Fox, *Gaussian 16, Revision C.01*, Gaussian, Inc., Wallingford CT, 2016.

17 M. Sugino, Y. Tsuchido, R. Maeda, I. Hisaki, H. Takano and H. Shinokubo, [3]CycloBODIPY: A Highly Strained Cyclic BODIPY Trimer with Effective Macrocyclic Conjugation, *Angew. Chem., Int. Ed.*, 2025, **64**, e202519612.

18 (*a*) V. I. Shcheslavskiy, M. V. Shirmanova, K. S. Yashin, A. C. Rück, M. C. Skala and W. Becker, Fluorescence Lifetime Imaging Techniques—A Review on Principles, Applications and Clinical Relevance, *J. Biophotonics*, 2025, **18**, e202400450; (*b*) C. Lim, D. Seah and M. Vendrell, Chemical Fluorophores for Fluorescence Lifetime Imaging, *Chem. Soc. Rev.*, 2026, **55**, 1352–1370.

19 (*a*) CCDC 2523317: Experimental Crystal Structure Determination, 2026, DOI: **10.5517/ccdc.csd.cc2qpqbh**; (*b*) CCDC 2523318: Experimental Crystal Structure Determination, 2026, DOI: **10.5517/ccdc.csd.cc2qpqcj**; (*c*) CCDC 2523319: Experimental Crystal Structure Determination, 2026, DOI: **10.5517/ccdc.csd.cc2qpqdk**.